Cell Calcium 35 (2004) 403–413

cell calcium

www.elsevier.com/locate/ceca

A model of the IP_3 receptor with a luminal calcium binding site: stochastic simulations and analysis

Daniel Fraiman*, Silvina Ponce Dawson

Departamento de Física, Facultad de Ciencias Exactas y Naturales, Universidad de Buenos Aires, Ciudad Universitaria, Pabellón I (1428), Buenos Aires, Argentina

Received 28 May 2003; received in revised form 20 August 2003; accepted 16 October 2003

Abstract

We have constructed a stochastic model of the inositol 1,4,5-trisphosphate receptor-Ca^{2+} channel that is based on quantitative measurements of the channel's properties. It displays the observed dependence of the open probability of the channel with cytosolic $[Ca^{2+}]$ and $[IP_3]$ and gives values for the dwell times that agree with the observations. The model includes an explicit dependence of channel gating with luminal calcium. This not only explains several observations reported in the literature, but also provides a possible explanation of why the open probabilities and shapes of the bell-shaped curves reported in [Nature 351 (1991) 751] and in [Proc. Natl. Acad. Sci. U.S.A. 269 (1998) 7238] are so different.

Keywords: $InsP_3$-receptor; Luminal Ca^{2+}; Stochastic model

1. Introduction

The inositol 1,4,5-trisphosphate (IP_3) receptor (IP_3R) is a ligand-gated intracellular Ca^{2+} release channel that plays a central role in modulating (free) cytoplasmatic Ca^{2+} concentration and which provides a link between events at the plasma membrane and Ca^{2+} release from intracellular stores. IP_3 receptors are regulated mainly by Ca^{2+}, IP_3 and ATP. Structurally, an IP_3R is composed of four subunits which form a single ion-conducting channel [3–5]. Three mammalian IP_3R subtypes (types I–III) are known. The subtypes are closely related (∼70% amino identity), but they are differentially expressed and differ in their affinities for IP_3 [6]. Most cells express several IP_3 subtypes, but they almost invariably express some type I receptors. The dynamic behavior of the IP_3R-ion channel has been studied by different methods. Bezprozvanny et al. [1] used reconstituted bilayers to obtain single channel records of the type I IP_3R, from which they could infer the (steady state) open probability. From these studies, they concluded that the open probability was an increasing function of $[IP_3]$ [7]. They also found that cytosolic Ca^{2+} played a dual role: while for relatively low cytosolic Ca^{2+} concentration ($[Ca^{2+}]_c$), the open probability was an increasing function of $[Ca^{2+}]_c$, it became a decreasing function for larger values of $[Ca^{2+}]_c$. The same type of behavior had already been observed in [8] and similar conclusions were drawn almost simultaneously in [9]. Qualitatively similar behaviors were also observed in experiments done on other cell types using different techniques (see, e.g. [2,10,11]).

Several models of the IP_3R have been presented in the literature to account for some of the experimental observations [12–14]. In particular, the De Young–Keizer model [12], was able to reproduce the open probability observed in [1], more specifically, its bell-shape as a function of $[Ca^{2+}]_c$. Recent experimental results [15] have challenged some of the features of the De Young–Keizer model. This disagreement might be attributed to the fact that the De Young–Keizer model was designed to fit the observations of a subtype of the IP_3R that is different from the one used in the experiments of [15]. However, there are various observations of the same subtype that report apparently conflicting results (see, e.g. [16]). For example, single channel records obtained using the patch-clamp technique on a native membrane (the membrane of the nucleus of a *Xenopus* oocyte) [2,10] have shown an open probability for the type I receptor that is an increasing function of $[IP_3]$ and that increases and decreases as a function of $[Ca^{2+}]_c$, but which has a shape that does

* Corresponding author. Tel.: +54-11-4576-3300; fax: +54-11-4576-3357.
E-mail address: dfraiman@df.uba.ar (D. Fraiman).

0143-4160/$ – see front matter © 2003 Elsevier Ltd. All rights reserved.
doi:10.1016/j.ceca.2003.10.004

not resemble the bell shape obtained in [1]. Furthermore, for similar [IP_3], the maximal open probability, as a function of [Ca^{2+}]$_c$, is very different: while this maximum value is around 0.15 in [1], it reaches the value 0.8 in [2]. The maximum open probability (P_o^{max}) for the type I receptor is also relatively large (∼0.5) in the experiments of [11]. In [2], a bell-shaped open probability may be observed but for IP_3 concentrations that are much lower than those used in [1]. As we argue in this paper, we think that these discrepancies could be due to the different luminal calcium concentrations that are used in the different experiments. We recognize that some of the observed differences might be due to the fact that some of the experiments use a native membrane while others use reconstituted planar bilayers, and this may result in the presence of different accessory proteins in both experimental types which might affect the kinetic behavior of the receptor. However, as we discuss later, we think that there is reasonable evidence for the plausibility of our hypothesis. Besides, it is important to mention that if we compare the open probabilities reported in [11] and in [1] there is a three-fold change in their maximum value, although both experiments are done using bilayers. Both experiments differ in the value of the luminal calcium concentration that is used. Furthermore, assuming that the kinetic properties of the receptor are affected by luminal calcium we are able to describe within a unified frameset not only these two types of experiments but also some recent observations obtained in experiments with ultralow luminal calcium [17].

Various experiments [11,16–20] suggest that the activity of the receptor depends on luminal calcium. In particular, the experimental results of [19] for the type I isoform imply that the open probability increases as [Ca^{2+}]$_{lum}$ decreases. This is in agreement with the experiments of [20] in which the open probability of the type I IP_3R is studied in planar bilayers for various values of [Ca^{2+}]$_{lum}$. The observations of [19,20] regarding the dependence of the open probability on luminal calcium are also compatible with more recent experiments reported in [17]. Finally, these observations also agree with those reported in [11] in which the maximum open probability is larger than the one in [1] (for similar [IP_3]), one of the differences between both experiments being [Ca^{2+}]$_{lum}$ (which is smaller in [11] than in [1]). Thus, one interpretation that is compatible with all these observations is to assume that the open probability depends on both [Ca^{2+}]$_{lum}$ and [Ca^{2+}]$_c$ in such a way that, for fixed [Ca^{2+}]$_c$, it is a decreasing function of [Ca^{2+}]$_{lum}$ (at least for a certain range of [Ca^{2+}]$_c$) and for fixed and low enough [Ca^{2+}]$_{lum}$ is an increasing function of [Ca^{2+}]$_c$ (up to very large values of [Ca^{2+}]$_c$).

To analyze whether the various results described before can be interpreted within a unified framework if luminal Ca^{2+} is taken into account, we develop in this paper a model of the IP_3R with a luminal calcium binding site. In this way, the gating of the receptor (and its open probability) is directly affected by [Ca^{2+}]$_{lum}$. This is not the first time that the existence of a luminal Ca^{2+} binding site has been proposed (see, e.g. [16]). However, we do not know of any actual mathematical implementation of a model with this feature. Therefore, our model provides the first mathematical test of what a luminal Ca^{2+} binding site could do.

2. Model and methods

2.1. The model

We show in Fig. 1 a schematic picture of the model we study in this paper, and, in Table 1, the parameter values for the various constants with which we could reproduce the experimental observations. As described in Section 1, one of the distinctive features of the model is the existence of a luminal Ca^{2+} binding site. For simplicity, we consider only one such binding site. Given the experimental observations, according to which the open probability is an increasing function of [IP_3] and is not a monotone function of [Ca^{2+}]$_c$, we also consider two cytosolic Ca^{2+} binding sites (one inhibitory and one activatory) and one IP_3 binding site, also on the cytosolic side.

The fact that, for fixed [Ca^{2+}]$_c$, the open probability decreases as [Ca^{2+}]$_{lum}$ is increased may be a consequence of a decreasing affinity of the inhibitory site with increasing [Ca^{2+}]$_{lum}$. The observation of [19] according to which high levels of intraluminal Ca^{2+} decrease the mean open time of the channel supports this possibility. Thus, we decided to develop a model in which the inhibitory cytosolic Ca^{2+} site is not available for binding all the time. Namely, the channel "shows" the inhibitory Ca^{2+} site on the cytosolic side only when the luminal calcium site is occupied. Thus, inhibition is hierarchically dependent on [Ca^{2+}]$_{lum}$ and [Ca^{2+}]$_c$ in our model: if [Ca^{2+}]$_{lum}$ is very low, then the channel will almost never inhibit, independently of the value of [Ca^{2+}]$_c$. In this way we can also explain the recent experiments described in [17] according to which the open probability remains high for [Ca^{2+}]$_c$ as high as 1 mM if [Ca^{2+}]$_{lum}$ is small enough.

The fact that certain sites are available for binding only after one ligand is bound to a particular site is characteristic of sequential models. Sequential models have been proposed in the past to describe the behavior of the IP_3R [15,21–23]. In [15,23], the availability of the Ca^{2+} binding sites depends on whether IP_3 is bound to the receptor or not. In the models of [21,22], which were introduced to describe Ca^{2+} waves, the inhibitory Ca^{2+} site is available for binding only after Ca^{2+} is bound to the activating site. As explained in [21], a choice for this type of kinetic model can be made if an actual conformation change occurs upon Ca^{2+} binding to the activating site or if Ca^{2+} binding to the activating site occurs so fast that it is very rare to encounter the receptor with Ca^{2+} bound to the inhibiting site but not to the activating site. The models of [21,22] are able to reproduce many of the observed features of Ca^{2+} waves. However, the open probability obtained in [22] does not change with cytosolic Ca^{2+} and IP_3 as it was later on observed experimentally (see,

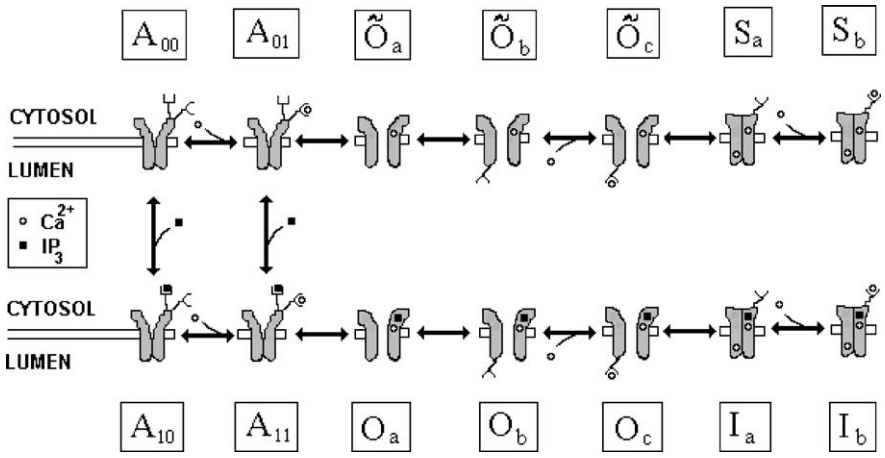

Fig. 1. Schematic picture of the states of the IP_3R and their transitions according to our model.

e.g. [2]). Namely, contrary to the observations, the value of $[Ca^{2+}]_c$ at which the maximum open probability occurs is an increasing function of $[IP_3]$ according to the model of [22]. This is due to an extra simplification introduced in that sequential model: the fact that the Ca^{2+} binding sites are available for binding only when IP_3 is bound to the receptor. The De Young–Keizer model, on the other hand, does predict the correct dependence of the maximum open probability with $[Ca^{2+}]_c$ and $[IP_3]$ [12]. This is a model which is not sequential at all in the sense that each site is available for binding independently of whether the others are occupied or not, and it is the existence of a state with Ca^{2+} bound to both the activating and the inhibiting sites which is ultimately responsible for the behavior of the maximum open probability described before. In the De Young–Keizer model the rate constant for IP_3 binding is much larger than that of Ca^{2+} binding to either the activating or the inhibiting sites. In spite of the disparity of reaction rates, a sequential model in which Ca^{2+} binding can occur only if IP_3 is bound cannot capture all the observed behaviors. This is so because the pace at which binding occurs also depends on the ligand concentration. Thus, if the choice of a sequential model is based on a timescale separation and the ligands that are involved in the various steps of the sequence are different, the timescale separation can cease to hold for certain concentrations. Sequential models are appealing because of their relative simplicity, however, the above discussion shows that their use is somewhat delicate. In our case, we tried to keep the model as simple as possible, which led us to organize certain steps in a sequential manner, even if the ligands could be different. However, we tried to reproduce a large variety of observations at the same time. Therefore, we tried to combine simplicity with the ability to reproduce as most observations as we could. Further experiments may prove that some of our current choices are wrong, but this is how the field can advance.

The IP_3R undergoes a large scale conformational change [4,5] upon switching from closed to open. Most previous models of the type I IP_3R, with some few exceptions [14,21,23] assume that conformation changes occur infinitely rapidly [12,13]. In these models there is a one to one correspondence between each state of the receptor and the occupation of the binding sites. Here we assume that major conformational changes take a finite time after ligand binding and unbinding. This is similar to models of the acetylcholine receptor [24]. In particular, the transition rate from the fully liganded state to the open state of the acetylcholine receptor estimated in [24] ($=0.714\,ms^{-1}$) is

Table 1
Transition probabilities of the model

Loop	ms^{-1}	O branch	ms^{-1}	Ô branch	ms^{-1}
$W[A_{01} \to A_{00}]$	0.022	$W[O_a \to O_b]$	0.133	$W[\hat{O}_a \to \hat{O}_b]$	0.5
$W[A_{10} \to A_{00}]$	Detailed balance	$W[O_b \to O_c]$	$0.07 \times [Ca^{2+}]_{lum}$	$W[\hat{O}_b \to \hat{O}_c]$	$5 \times [Ca^{2+}]_{lum}$
$W[A_{11} \to A_{10}]$	0.667	$W[O_c \to I_a]$	1.6	$W[\hat{O}_c \to S_a]$	5
$W[A_{11} \to A_{01}]$	0.018	$W[I_a \to I_b]$	$0.06 \times [Ca^{2+}]_c$	$W[S_a \to S_b]$	$5 \times [Ca^{2+}]_c$
$W[A_{00} \to A_{01}]$	$5 \times [Ca^{2+}]_c$	$W[I_b \to I_a]$	0.01	$W[S_b \to S_a]$	0.02
$W[A_{00} \to A_{10}]$	$6.67 \times [IP_3]$	$W[I_a \to O_c]$	0.4	$W[S_a \to \hat{O}_c]$	0.25
$W[A_{10} \to A_{11}]$	$0.5 \times [Ca^{2+}]_c$	$W[O_c \to O_b]$	2	$W[\hat{O}_c \to \hat{O}_b]$	0.15
$W[A_{01} \to A_{11}]$	$6.67 \times [IP_3]$	$W[O_b \to O_a]$	1.5	$W[\hat{O}_b \to \hat{O}_a]$	0.1
$W[A_{11} \to O_a]$	0.55	$W[O_a \to A_{11}]$	0.33	$W[\hat{O}_a \to A_{01}]$	0.5
$W[A_{01} \to \hat{O}_a]$	0.00035				

All concentrations in μM.

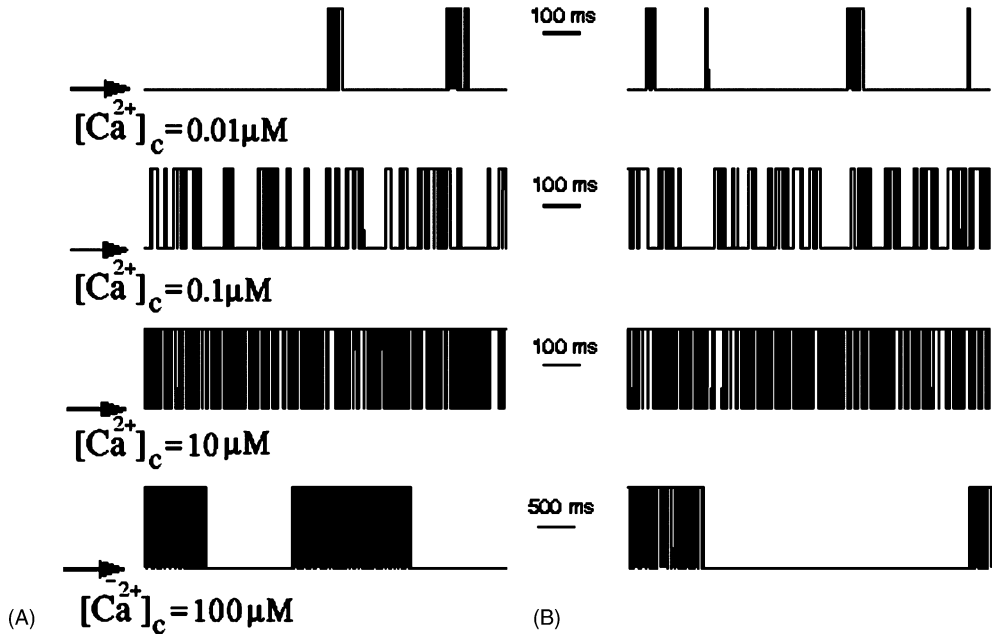

Fig. 2. Simulated IP_3R channel current for $[Ca^{2+}]_{lum} = 0.3\,\mu M$, $[IP_3] = 10\,\mu M$, and various values of $[Ca^{2+}]_c$. Arrows indicate the zero current level. We observe that, while $[Ca^{2+}]_c$ does not exceed a threshold value, the channel opens more frequently as $[Ca^{2+}]_c$ is increased and when $[Ca^{2+}]_c$ is increased beyond the threshold value, the frequency of openings starts to decrease. In (A) the states $\{\hat{O}_a, \hat{O}_b, \hat{O}_c\}$ are treated as open and in (B) they are treated as closed. For each value of $[Ca^{2+}]_c$ used in this figure, the records in (A) and (B) are statistically equivalent. The differences in the current traces are manifest only for very low $[IP_3]$.

of the same order of magnitude as the transition rate describing the conformation change to the most relevant open state of our model ($W[A_{11} \rightarrow O_a]$ in Table 1). We assume that these transitions between conformations are modulated by ATP, but the simulations we present here are done with fixed $[ATP] = 500\,\mu M$. We will discuss ATP modulation in a future paper.

Recent experiments indicate that the channel can open in the absence of IP_3 for low enough $[Ca^{2+}]_c$ [25]. This result can be incorporated within the model or not depending on whether the $\hat{O}$ states of the model correspond to open or closed conformations. In agreement with the experimental observations, the probability that the channel is in one of the $\hat{O}$ states is quite low. Thus, most of the single channel records that the model generates are insensitive to whether the $\hat{O}$ states are treated as open or closed (see Fig. 2). The primary features of the model we present here are the luminal Ca^{2+} binding site and the finite transition rates between major conformations. If these primary features hold up, then future experiments can be used to settle delicate questions such as whether the $\hat{O}$ states should be treated as open or closed.

We see in Fig. 1 that, in the unliganded conformation (A_{00}), only the IP_3 and the activatory Ca^{2+} binding sites are available for binding. If these two sites are occupied (A_{11}) then the channel can make a transition to one of its open conformations (O_a). From this state, the channel can further change its conformation exposing, then, the regulatory Ca^{2+} binding site to the luminal side (state O_b). If a Ca^{2+} ion binds to this site, then, the channel can close. As before, we assume that the pore does not close immediately upon binding but rather that the ligand promotes a conformation change to a closed or inhibited state, I_a. As depicted in Fig. 1, when the channel is in the I_a state, the inhibitory cytosolic Ca^{2+} site becomes available for binding. It is important to stress that before this cytosolic site becomes "exposed" the channel is closed. The implication of this choice is discussed later. As shown in Fig. 1, the model has two branches, one "born" from the A_{11} state that comprises the states mentioned before, and the other one that branches off the A_{01} state (one Ca^{2+} bound to the activating site). The space of states that branches off the A_{01} state is similar to the one that starts from A_{11}, but with very different rate constants.

Before deciding to work with the model of Fig. 1 we also studied the behavior of a similar model but with the "second branch" starting on the A_{00} state rather than the A_{01} state. Most of the results that we show in the following section about the open probability and mean open and closed times remained unaffected with the exception of one: the $[IP_3]$ dependence of the value of $[Ca^{2+}]_c$ ($[Ca^{2+}]_c^{max}$) at which the maximum open probability occurs. This value of $[Ca^{2+}]_c$ only increases with $[IP_3]$, in agreement with the experiments, in the model with the second branch starting from the A_{01} state. This is why we decided to keep the model of Fig. 1.

2.2. Numerical simulations

In order to probe the ability of the model to reproduce the observations, we simulated the Markov process whose state space is described by Fig. 1, using continuous time with a resolution of 0.1 ms. The stochastic procedure is as follows.

Assume that at time t the channel enters the A_{00} state. Two possible transitions can occur: to state A_{01} (if cytosolic Ca^{2+} binds to the IP_3R), with transition probability per unit time $W[A_{00} \to A_{01}]$ and to state A_{10} (if IP_3 binds to the IP_3R), with transition probability per unit time $W[A_{00} \to A_{10}]$. In order to decide which transition occurs and at what time, we take the minimum of two exponentially distributed random variables: t_1, with mean $1/W[A_{00} \to A_{01}]$ and t_2, with mean $1/W[A_{00} \to A_{10}]$. For example, if $t_2 = \min\{t_1, t_2\} = 10.5$ ms, then the channel stays in state A_{00} for 10.5 ms after which it makes a transition to the A_{01} state. The transition probabilities we use are in Table 1. We chose these values so that the model gives results similar to the experimental observations of [2,26] for $[Ca^{2+}]_{lum} = 0.3\,\mu M$, $[ATP] = 0.5$ mM, $[IP_3] = 10\,\mu M$ and various values of $[Ca^{2+}]_c$. The values of the concentrations, $[IP_3]$, $[Ca^{2+}]_{lum}$, $[Ca^{2+}]_c$, were chosen for each simulation depending on the experiment that we were trying to simulate.

We show in Fig. 2 some of the time series we obtained from our stochastic simulations for $[IP_3] = 10\,\mu M$, $[Ca^{2+}]_{lum} = 0.3\,\mu M$ and various $[Ca^{2+}]_c$, assuming the same (fixed) current for all open states. The traces shown in (A) were generated assuming the $\hat{O}$ states are open. Those in (B) were generated assuming the $\hat{O}$ states are closed. For these values of IP_3 and $[Ca^{2+}]_c$, the current records obtained in both cases are statistically equivalent. As discussed previously, most of the single channel records that the model generates are insensitive to whether the $\hat{O}$ states are treated as open or closed. The main difference occurs for low $[Ca^{2+}]_c$ in the absence of IP_3. In such a case, if the $\hat{O}$ are treated as open then the model channel opens for very low $[Ca^{2+}]_c$ in the absence of IP_3. If they are treated as closed the model will not open under those conditions.

2.3. Statistics

The stationary open probability can be found analytically from the master equations of the model. We show the results of that calculation in most of the figures, and, in some of them, the one that can be estimated by averaging over several (usually 3) stochastic simulations. In the case of the mean open and closed times we present the results from the stochastic simulations only.

3. Results

3.1. Open probability: $[Ca^{2+}]_c$ and $[IP_3]$ modulation

We show in Fig. 3, the stationary open probability as a function of $[Ca^{2+}]_c$ for various $[IP_3]$ (100, 10, 1 μM, 100 and 10 nM) and for fixed $[Ca^{2+}]_{lum} = 0.3\,\mu M$ (solid lines). For the sake of comparison, we also show the results from the stochastic simulations for $[IP_3] = 100\,\mu M$ (symbols). The way the maximum open probability, P_o^{max}, changes with $[IP_3]$ is similar to the one reported in [2,7]. Namely, as observed in those papers, P_o^{max} increases with $[IP_3]$ until it reaches a saturating value. The value of $[Ca^{2+}]_c$ at which $P_o([Ca^{2+}]_c, [IP_3]) = P_o^{max}$ also behaves as observed in the experiments. Namely, it increases with $[IP_3]$. Furthermore, the values of Fig. 3 are very similar to the data reported in [2], for the same $[Ca^{2+}]_{lum}$.

Recent experiments done using lipid bilayers have shown that mutants of the IP_3R with lower affinity for Ca^{2+} in the putative Ca^{2+} sensor region also display a bell-shaped open probability as a function of $[Ca^{2+}]_c$ [27] but where both the $[Ca^{2+}]_c$ at which $P_o = P_o^{max}$ and the range of $[Ca^{2+}]_c$ for which P_o is non-negligible correspond to larger

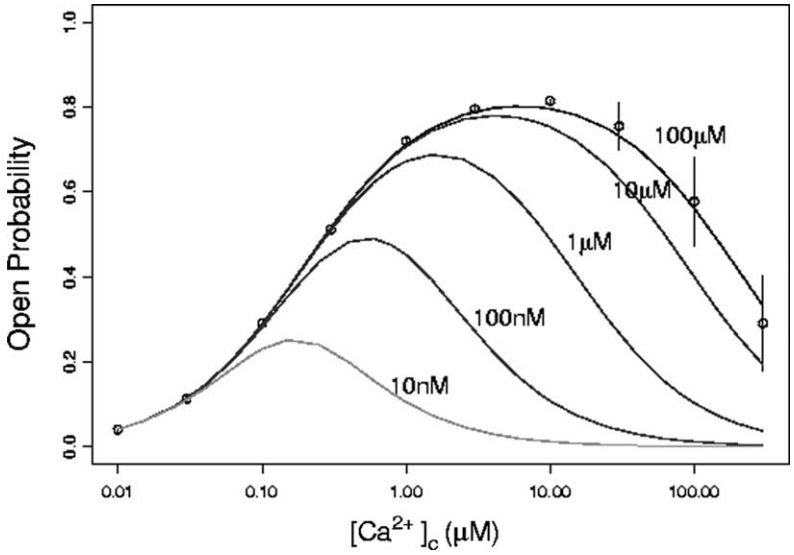

Fig. 3. Open probability as a function of $[Ca^{2+}]_c$ for $[IP_3] = 100$, 10, 1 μM, 100 and 10 nM. We show in all cases the analytically obtained stationary probability (solid line). For $[IP_3] = 100\,\mu M$, we also show the mean and standard deviation over 3 realizations of the stochastic model (circles).

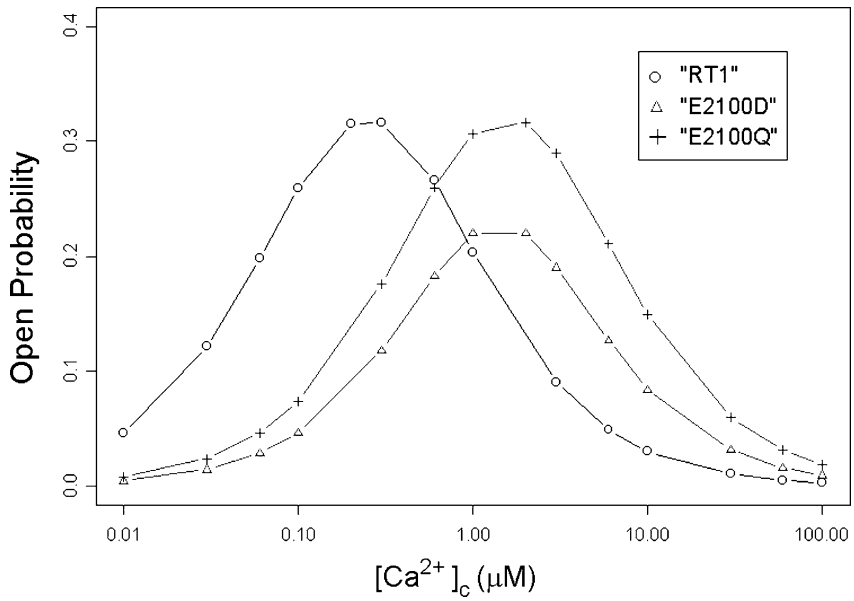

Fig. 4. Open probability as a function of $[Ca^{2+}]_c$ for $[IP_3] = 100\,\mu M$ and $[Ca^{2+}]_{lum} = 100\,\mu M$. The circles correspond to realizations obtained with the parameters of Table 1, while the crosses and triangles correspond to realizations obtained by changing the cytosolic Ca^{2+} binding parameters. The notation is the same as in [27].

$[Ca^{2+}]_c$ values than those of the wild type. Our model is able to reproduce this observation. In fact, if we use $[IP_3] = 100\,\mu M$, $[Ca^{2+}]_{lum} = 100\,\mu M$, and decrease $W[A_{00} \rightarrow A_{01}]$, $W[A_{10} \rightarrow A_{11}]$, $W[S_a \rightarrow S_b]$, $W[I_a \rightarrow I_b]$, by a factor of six, the open probability curve shifts to the right, having its maximum at $[Ca^{2+}]_c \approx 2\,\mu M$ as observed in [27]. Meanwhile P_o^{max}, as shown in Fig. 4, can either remain constant (as in the case of the E2100Q mutation) or decrease (as in the case of the E2100D mutation) depending on whether the factors by which the probability of binding to the activatory and to the inhibitory sites are decreased are the same (E2100Q) or lightly differ between themselves (E2100D).

We show in Fig. 5, the open probability obtained from our stochastic simulations (each cross representing a single simulation) in the absence of IP_3, and the stationary open probability obtained analytically from the model (solid line) if the $\hat{O}$ states are assumed to be open. As may be observed, in accordance with the reports of [25], the open probability is very low and only significant for very low $[Ca^{2+}]_c$ ($[Ca^{2+}]_c < 100\,nM$). This supports our previous statement

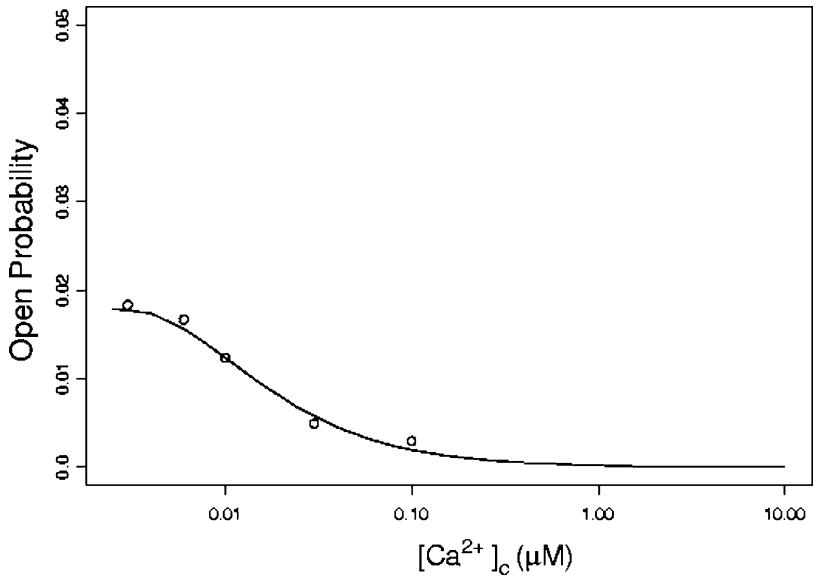

Fig. 5. Open probability as a function of $[Ca^{2+}]_c$ for zero IP_3. Results from individual stochastic simulations (circles) and stationary probability obtained analytically from the model (solid line).

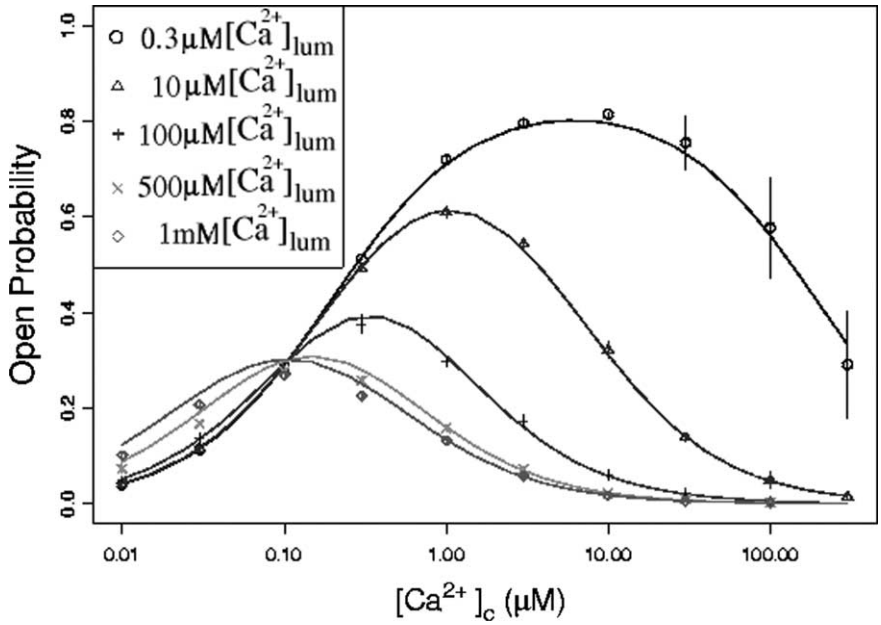

Fig. 6. Open probability as a function of $[Ca^{2+}]_c$ in the presence $[IP_3] = 10\,\mu M$ for various values of $[Ca^{2+}]_{lum}$. Mean and standard deviation over three realizations (symbols) and analytical stationary open probability (solid line).

according to which whether the $\hat{O}$ states are considered to be open or closed states does not change the results on the open probability at the $[IP_3]$ levels typically used in experiments.

3.2. Open probability: $[Ca^{2+}]_c$ and $[Ca^{2+}]_{lum}$ modulation

In this section, we discuss the model's dependence on $[Ca^{2+}]_{lum}$. We show in Fig. 6 the stationary open probability as a function of $[Ca^{2+}]_c$ for various values of $[Ca^{2+}]_{lum}$ and $[IP_3] = 100\,\mu M$. There we observe that the maximum open probability, P_o^{max}, gets smaller as $[Ca^{2+}]_{lum}$ is increased, and that the value of $[Ca^{2+}]_c$ that maximizes the open probability, $[Ca^{2+}]_c^{max}$, becomes smaller as $[Ca^{2+}]_{lum}$ is increased. The behavior of $[Ca^{2+}]_c^{max}$ with $[Ca^{2+}]_{lum}$ is consistent with the observations reported in Fig. 3 of [11] where the authors compare the open probability of [1] with the one they obtain, for the type I receptor, using a smaller $[Ca^{2+}]_{lum}$. We also observe in Fig. 6 that the open probability curve becomes more "bell-shaped" and narrower as $[Ca^{2+}]_{lum}$ increases. In particular, the curve we obtain for $[Ca^{2+}]_{lum} = 0.3\,\mu M$ is very similar to the experimental one reported in [2] for this value of $[Ca^{2+}]_{lum,}$ while the one we obtain for $[Ca^{2+}]_{lum} = 100\,\mu M$ resembles the experimental one of [1], obtained for $[Ca^{2+}]_{lum} \sim 50\,mM$. We also observe in Fig. 6 that, for large luminal calcium concentrations ($[Ca^{2+}]_{lum} > 300\,\mu M$), the receptor becomes "more sensitive" to $[Ca^{2+}]_c$ (there is activity for $[Ca^{2+}]_c = 10\,nM$).

Although this has not been studied at the single channel level, other types of studies show results that agree with this last observation. Namely, in [18], where a superfusion protocol is used with permeabilized A7r5 smooth muscle cells, the authors observe a big response (large calcium release) if the stores are fully loaded (3400 pmol $Ca^{2+}/10^6$ cells), even if $[Ca^{2+}]_c$ is as low as 10 nM, which is consistent with our observation of Fig. 6. Missiaen et al. [18] conclude that the channel opens in the presence of IP_3 even in the lack of cytosolic calcium if $[Ca^{2+}]_{lum} = 1$ or 0.6 mM.

We finally investigated the behavior of the model for ultralow luminal calcium. We show in Fig. 7 the open probability for $[Ca^{2+}]_{lum} = 1\,nM$, and three values of $[IP_3] = 1$, 100 nM, and 10 μM. There we can see that the channel does not inhibit at high cytosolic calcium concentration, which agrees with the description of [17]. This observation naturally fits in our picture according to which the shape of the open probability curve as a function of $[IP_3]$ depends on $[Ca^{2+}]_{lum}$.

3.3. Mean open and closed times

Analysis of open and closed dwell time distributions provide information on rate constants. By contrast, the stationary open probability provides only equilibrium constants. Dwell time distributions have been obtained in [28] where it is shown that the mean open time, $\langle \tau_o \rangle$, lies within a narrow range with negligible dependence on $[Ca^{2+}]_c$ between $[Ca^{2+}]_c = 100\,nM$ and 50 μM in saturating IP_3, while in the tails ($[Ca^{2+}]_c < 100\,nM$ or $[Ca^{2+}]_c > 50\,\mu M$) the mean open time is smaller. The dwell time distribution can be biased due to limitations in the temporal resolution of the records. If the nonmonotonic behavior of $\langle \tau_o \rangle$ as a function of $[Ca^{2+}]_c$ is real (and not due to the time resolution), then there is a problem: most theoretical models of the IP_3R [12–15] cannot reproduce this behavior. For example, if we consider the working model of Adkins and Taylor [15], ac-

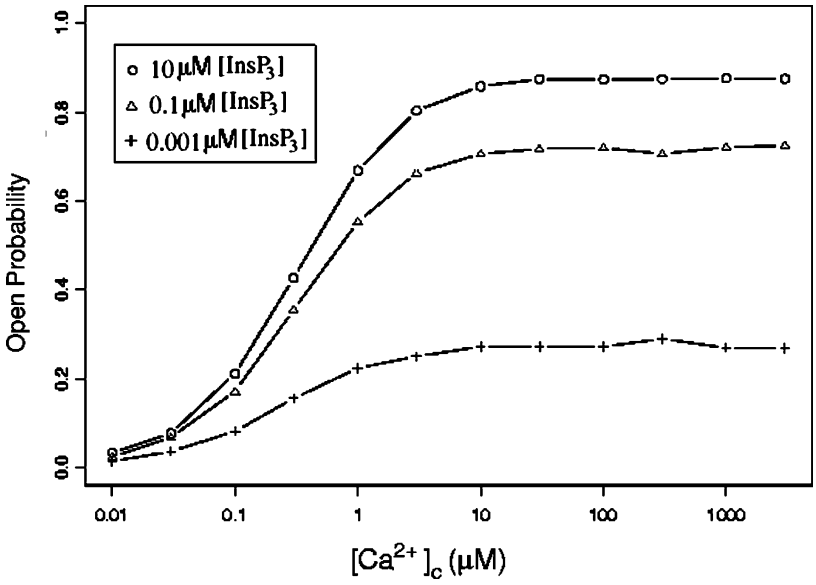

Fig. 7. Open probability as a function of $[Ca^{2+}]_c$ in the presence of $[Ca^{2+}]_{lum} = 1\,nM$, for $[IP_3] = 10\,\mu M$, 100 and 1 nM.

cording to which the only allowed transitions from the open state involve losing a ligand, then the (well resolved) $\langle\tau_o\rangle$ should be concentration-independent. On the other hand, in all other models in which the receptor can also "leave" the open state by binding Ca^{2+} to an inhibitory site, $\langle\tau_o\rangle$ should be a monotonically decreasing function of $[Ca^{2+}]_c$. Our model with four binding sites would also behave in this way. However, we have done some preliminary work [29] that shows that the experimental type of response observed in [28] can be obtained if the channel is considered to be formed by four subunits, each of which is described by a model like the one in Fig. 1 (with rate constants different from those of Table 1). This way of solving this problem also provides a means by which subconductances can be studied. Thus, although our simple model predicts that $\langle\tau_o\rangle$ is monotone with $[Ca^{2+}]_c$, it is easy to modify it in order to reproduce the experimental behavior [29].

In spite of the limitations of the four binding site model, we are interested in analyzing whether it can display other features of the dwell time distributions, in particular, the behavior of the mean open time with luminal calcium. To this end, we show in Fig. 8 the mean open time, $\langle\tau_o\rangle$, as a function of $[Ca^{2+}]_c$ obtained from simulations with $[Ca^{2+}]_{lum} =$ 0.3, 10, 100, 500, 1000 μM. We can see that $\langle\tau_o\rangle$ is monotone with $[Ca^{2+}]_c$, this agrees with the experimental observations of [2,28], except for the tails. Also it is interesting to note that $\langle\tau_o\rangle$ decreases when $[Ca^{2+}]_{lum}$ is increased, until it reaches a saturating value (data not shown). The time it takes for the channel to expose the intraluminal Ca^{2+} binding site once it is open (which is determined by the transition rate $W[O_a \rightarrow O_b]$) and the time it takes to make the conformational change once Ca^{2+} binds to the luminal site (determined by the transition rate $W[O_c \rightarrow I_a]$) are responsible for this saturating time. The mean open time obtained by Bezprozvanny and Ehrlich using $[Ca^{2+}]_{lum} \sim 50\,mM$ ($\langle\tau_o\rangle \approx 3\,ms$ [19]) is smaller than the one obtained by Mak et al. using $[Ca^{2+}]_{lum} \sim 500\,nM$ ($\langle\tau_o\rangle \approx 6\,ms$ [28]). Our model does display values of $\langle\tau_o\rangle$ that decrease when $[Ca^{2+}]_{lum}$ is increased, but the values we obtain are a little bit smaller than the experimentally observed ones (3.3 ms instead of 6 ms and 2 ms instead of 3 ms). However, it is important to remember that we are working with a time resolution of 0.1 ms. If the time-series were binned at 0.2 ms (5 kH), the mean open times would get closer to the experimentally observed ones. The mean closed time, on the other hand, has a "u-shaped" dependence on $[Ca^{2+}]_c$, achieving its minimum value at the value of $[Ca^{2+}]_c$ at which the open probability is maximum. For $[Ca^{2+}]_{lum} = 300\,nM$, the smallest mean closed time is 1 ms and occurs at $[Ca^{2+}]_c =$ 10 μM. This time is similar to the one observed by the group of Foskett's [2,28] (≈2 ms at $[Ca^{2+}]_c \approx 10\,\mu M$). As we in-

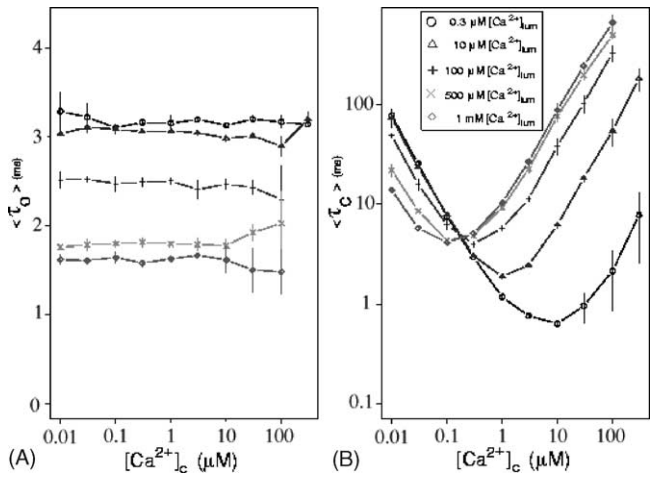

Fig. 8. $[Ca^{2+}]_c$ dependence of the mean open, $\langle\tau_o\rangle$, (A) and closed, $\langle\tau_c\rangle$, (B) times of the IP_3R.

crease the value of $[Ca^{2+}]_{lum}$ the smallest mean closed time increases, just opposite to what occurs with the mean open times. We also remark on two important results. First the distribution of the open and closed times (dwell times), are not single exponentials in agreement with the experimental observations in [28]. Second, the mean open times do not depend on the IP_3 concentration. This agrees with the observations reported by Hagar and Ehrlich for the type III IP_3R in [30]. These data will be analyzed in more detail elsewhere.

4. Discussion

The IP_3R plays a central role in modulating the free Ca^{2+} concentration inside cells. Therefore, it is of utmost importance to unveil the way it works. Single channel records obtained from a variety of experiments have reported apparently conflicting results. We have focused primarily on the differences in the maximum open probability observed in [1,11,20] and [2,28] for similar values of IP_3 and cytosolic Ca^{2+} concentrations and on the shape that the open probability curve displays as a function of $[Ca^{2+}]_c$ for various values of $[IP_3]$. We have introduced a model of the IP_3R with a luminal Ca^{2+} binding site which can account for the apparent discrepancies among these experimental observations. Moreover, by varying $[Ca^{2+}]_{lum}$ we have been able to reproduce the main features of the experiments presented in [2,11,28] and [1], showing that their differences can be explained in terms of the different luminal calcium concentrations used by the different groups.

Various experiments [11,16–20] had already suggested that the activity of the channel also depends on luminal calcium. More specifically, the results of [19] implied that the open probability increased as $[Ca^{2+}]_{lum}$ decreased. As stated by the authors: "high levels of intraluminal Ca^{2+} inhibit ip-gated channels by decreasing both the frequency of channel openings and the mean open time of the channels" [19]. The results of [19] agree with those of [20], where the authors state that "in contrast to the data at 1 mM trans (luminal) Ca^{2+}, the channel at 300 nM trans Ca^{2+} shows much less spontaneous inactivation, longer open times, and a higher conductance as well as multiple conductances states". These observations are compatible with those of [17] in which the authors report that exposure of the nuclei they use for their patch-clamp experiments to ultralow calcium concentrations prevents the receptor from being inhibited at high cytosolic calcium concentrations (even as high as 1.5 mM). The bath solution in these experiments is believed to be in equilibrium with the solution on the luminal side of the receptor [2]. Therefore, this "lack of inhibition" could be attributed to the use of a very low $[Ca^{2+}]_{lum}$. Finally, all these observations also agree with the results of [11] which show a larger maximum open probability than the one in [1] (for similar $[IP_3]$), whereas they use a smaller $[Ca^{2+}]_{lum}$.

Assuming that luminal Ca^{2+} is directly implicated on the gating of the channel is not the only possibility to describe a decreasing open probability with $[Ca^{2+}]_{lum}$. In fact, Bezprozvanny and Ehrlich presented a skeletal model in which the effect of $[Ca^{2+}]_{lum}$ on channel gating is mediated by the Ca^{2+} current that crosses the channel once it is open [19]. Namely, if the experiment is done in conditions such that the Ca^{2+} current flows from the luminal to the cytosolic side (and this is the case in the experiments reported in [19]), then the local $[Ca^{2+}]_c$ near the channel's mouth will remain higher than in the bulk as long as the channel remains open. The receptor will then sense this local $[Ca^{2+}]_c$ and most probably will close (if the local $[Ca^{2+}]_c$ is higher than the value at which the open probability switches from being an increasing to being a decreasing function of $[Ca^{2+}]_c$). Although this type of model could easily explain the fact that the mean open time should decrease with increasing $[Ca^{2+}]_{lum}$, it is not clear how it could explain the smaller frequency of channel openings reported in [19]. Besides, it cannot explain the observations of [20] or of [17], in which the experiments are done in such a way that K^+ rather than Ca^{2+} is the ion carrier, exactly to prevent calcium induced calcium release from occurring.

One of the properties that complicates the study of the IP_3R is the fact that it is mainly a Ca^{2+} channel and Ca^{2+} is one of its agonists. Therefore, the way the channel works will be affected by the ionic current that traverses it (unless this current lacks Ca^{2+}). It is for this reason that Mak et al. and other groups [11] do their experiments with very low $[Ca^{2+}]_{lum}$, measuring monovalent cation (K^+ or Cs^+) rather than Ca^{2+} currents. Ehrlich's group, on the other hand, use divalent cations other than Ca^{2+} (Ba^{2+}, Sr^{2+}, Mg^{2+}), to which the channel is permeable [19,30]. The rationale behind these choices makes sense if Ca^{2+} binding sites are only available on the cytosolic side. For example, for most of the experiments of Mak et al., if there is any Ca^{2+} current, it should flow from the cytosolic to the luminal side (Bezprozvanny and Ehrlich mention in [19] that they do not observe current flowing from the cytosolic to the luminal side). Such a current would not affect the local $[Ca^{2+}]_c$ (provided that the local depletion that the current may cause is replenished by diffusion fast enough) and so the experiment would correspond to the known bulk concentration. However, it would affect the calcium concentration on the luminal side. If there is an intraluminal Ca^{2+} binding site, this Ca^{2+} current would then affect the open probability of the channel. We do not know of any report of such an observation. In the simulations we have presented in this paper we have not considered the formation of Ca^{2+} microdomains on either side of the membrane. Namely, we have done the simulations assuming constant values of $[Ca^{2+}]_c$ and $[Ca^{2+}]_{lum}$. We think that, for our model, the effect of microdomain formation on the cytosolic side will not be significant because the inhibitory cytosolic Ca^{2+} site is present only after the channel has already closed. In the case of the luminal side, we did not include

such an effect because there was no experimental observation to support it.

Having a model with a luminal Ca^{2+} binding site allowed us to obtain both a bell shape (as observed in [1]) and a more "square-like" (as observed in [2]) dependence of the open probability with $[Ca^{2+}]_c$, depending on the value of $[Ca^{2+}]_{lum}$, as shown in Fig. 6. This observation together with the fact that, in our model, both P_o^{max} and the value of $[Ca^{2+}]_c$ at which it occurs, $[Ca^{2+}]_c^{max}$, get smaller as $[Ca^{2+}]_{lum}$ is increased supports our idea that the difference in the open probabilities observed in [1] and [2,26] can be due to the different values of $[Ca^{2+}]_{lum}$ used in the experiments. Furthermore, the transition from a "bell-shape" open probability to a more "square" dependence with $[IP_3]$ as $[Ca^{2+}]_{lum}$ is decreased allows us to fit quite naturally the recent observations reported in [17] on the lack of inhibition of the IP_3R for pretty large $[Ca^{2+}]_c$ in ultralow $[Ca^{2+}]_{lum}$ (see Fig. 7). The luminal Ca^{2+} binding site also allows us to interpret, in a simple way, the results of [19] on the way the channel behaves when divalent ions other than Ca^{2+} are used as carriers. In that paper, the ions used were: Ca^{2+}, Mg^{2+}, Sr^{2+} and Ba^{2+}. From these studies the authors observed that the mean open time was the smallest when Ca^{2+} was the carrier ($\langle\tau_{open}^{Ca^{2+}}\rangle = 2.9\,ms$, $\langle\tau_{open}^{Mg^{2+}}\rangle = 4.3\,ms$, $\langle\tau_{open}^{Sr^{2+}}\rangle = 5.9\,ms$, and $\langle\tau_{open}^{Ba^{2+}}\rangle = 6.4\,ms$). This observation can be interpreted in terms of our model in the following way. If we think that the calcium luminal site is quite selective for calcium, then when there is Ca^{2+} on the luminal side, the receptor will jump more quickly from the open to the inhibited state than when other divalent ions are present in the same concentration. If this transition occurs more quickly, then the mean open time will be smaller and the open probability will also be affected.

We have built a model with a luminal Ca^{2+} binding site mainly to explain the apparent discrepancies between some experiments. Now, one could argue that the differences observed in [1] and [2] could be due to the use of different cell types and/or experimental techniques, in such a way that accessory proteins that may affect channel gating [31] could be present in one experiment and absent in the other one. However, the maximum open probability reported in [11] and in [1] is quite different for similar values of $[IP_3]$ and $[Ca^{2+}]_c$, while the experiments are done, in both cases, with reconstituted bilayers from cerebellum. We think that this discrepancy provides strong evidence in favor of our argument. There are still some discrepancies that we have not solved. For example, the experiments of [11] and [2] use similar values of $[Ca^{2+}]_{lum}$, however, they observe a different value of P_o^{max}, albeit, larger, in both cases, than the one of [1]. In this case, the small difference in P_o^{max} could perhaps be attributed to the lack of accessory proteins in one of the experiments.

We have constructed our model based on a variety of observations. However, there are many more observations that we did not take into account. In particular, there are several experimental studies that are done in intact cells in which Ca^{2+} release through IP_3R's is observed using optical techniques (see, e.g. [32–34]). In these experiments there are several factors that are acting simultaneously and a complete mathematical description of the observations requires not only a model of the IP_3R, but also a model of Ca^{2+} diffusion in the presence of buffers [35], the effect of Ca^{2+} on nearby receptors and, possibly, the effect of counter-ions [36]. To some extent, something similar occurs with superfusion experiments [9,15], although some of these effects could be ruled out. In order to determine how the IP_3R-channel works we think that it is best to first develop a model based on tightly controlled single channel records. We assume that the experiments that provide these data reflect the intrinsic dynamical properties of the IP_3R and build a model accordingly, even if some of them are done for aphysiological concentrations. We have built our model based on this concept.

Although we have shaped our model based on a variety of experimental observations, additional experiments would be helpful in order to decide whether the basic structure we propose is correct or not. In particular, a systematic study of the dependence of the open probability on $[Ca^{2+}]_{lum}$ (for the different experimental protocols with which the IP_3R has been studied) would serve to validate or not the main point we try to make with our model. Namely, the fact that the discrepancies observed in the different types of experiments are related to the difference in the amount of Ca^{2+} used on the luminal side. A detailed analysis of dwell time distributions as a function of $[Ca^{2+}]_{lum}$ would also help in this regard. Finally, a detailed analysis of experiments with very low $[Ca^{2+}]_{lum}$ ($<1\,nM$) and large $[Ca^{2+}]_c$ ($>1\,\mu M$) would be useful to validate the existence of an open state on the branch that starts from the A_{01} state.

In this paper, we tried to describe a variety of observations within a unified model, but, at the same time, we tried to keep the model as simple as possible. Mainly we tried to answer the very basic question of which are the agonists (cytosolic and/or luminal) that affect channel gating. While we could reproduce some of the observations quantitatively, in other cases the model only gave a qualitative agreement. New experiments should be done to further test the main features of our model, in particular, the effect of luminal Ca^{2+} on channel gating. From a modeling point of view, we see our model as a necessary step from which more sophisticated models may be built. In particular, we think that advancing in a direction in which the tetrameric structure of the receptor is taken into account might explain some of the reported observations on the mean open time of the channel.

Acknowledgements

We acknowledge useful conversations with D. Mak, K. Foskett, I. Parker and J. Pearson. This work has been funded by Universidad de Buenos Aires, ANPCyT-Argentina (PICT 03-08133) and National Institutes of Health (GM65830).

S.P.D. is member of Carrera del Investigador Científico (CONICET).

References

[1] I. Bezprozvanny, J. Watras, B.E. Ehrlich, Bell-shaped calcium-response of Ins(1,4,5)P3—and calcium-gated channels from endoplasmic reticulum of cerebellum, Nature 351 (1991) 751–754.

[2] D.-O.D. Mak, S. McBride, J.K. Foskett, Inositol 1,4,5-tris-phosphate activation of inositol tris-phosphate receptor Ca^{2+} channel by ligand tuning of Ca^{2+} inhibition, Proc. Natl. Acad. Sci. U.S.A. 269 (1998) 7238–7242.

[3] C.C. Chadwick, A. Saito, S. Fleisher, Inositol 1,4,5-trisphophate receptors: distinct neuronal and nonneuronal forms derived by alternative splicing differ in phosphorylation, Proc. Natl. Sci. U.S.A. 88 (1991) 2951–2955.

[4] Q.X. Jiang, E.C. Thrower, D.W. Chester, B.E. Ehrlich, F.J. Sigworth, Three-dimensional structure of the type 1 inositol 1,4,5-trisphosphate receptor at 24 AA resolution, EMBO J. 21 (2002) 3575–3581.

[5] K. Hamada, T. Miyata, K. Mayanagi, J. Hirota, K. Mikoshiba, Two-state conformational changes in inositol 1,4,5-trisphosphate receptor regulated by calcium, JBC 277 (2002) 21115–21118.

[6] H. Yoneshima, A. Miyawaki, T. Michikawa, T. Furichi, K. Mikoshiba, Ca^{2+} differentially regulates the ligand-affinity states of type 1 and type 3 inositol 1,4,5-trisphosphate receptors, Biochem. J. 322 (1997) 591–596.

[7] J. Watras, I. Bezprozvanny, B.E. Ehrlich, Inositol 1,4,5-triphosphate-gated channels in cerebellum—presence of multiple conductance states, J. Neurosci. 11 (1991) 3239–3245.

[8] M. Iino, Biphasic calcium dependence of inositol trisphosphate induced calcium release in smooth muscle cells of the guinea pig *Taenia caeci*, J. Gen. Physiol. 95 (1990) 1103–1122.

[9] E.A. Finch, T.J. Turner, et al., Calcium as a co-agonist of inositol 1,4,5-trisphosphate-induced calcium release, Science 252 (1991) 443–446.

[10] D.-O.D. Mak, J.K. Foskett, Single-channel kinetics, inactivation and spatial distribution of inositol trisphosphate (IP3) receptors in *Xenopus* oocyte nucleus, J. Gen. Physiol. 109 (1997) 571–587.

[11] J. Ramos-Franco, M. Fill, G.A. Mignery, Isoform-specific function of single inositol 1,4,5-trisphosphate receptor channels, Biophys. J. 75 (1998) 834–839.

[12] G.W. De Young, J. Keizer, A single-pool inositol 1,4,5-triphosphate-receptor-based model for agonist-stimulated oscillations in Ca^{2+} concentration, Proc. Natl. Acad. Sci. U.S.A. 89 (1992) 9895–9899.

[13] S. Swillens, L. Combettes, P. Champeil, Transient inositol 1,4,5-trisphosphate-induced Ca^{2+} release: a model based on regulatory Ca^{2+}-binding sites along the permeation pathway, Proc. Natl. Acad. Sci. U.S.A. 91 (1994) 10074–10078.

[14] I.I. Moraru, E.J. Kaftan, B.E. Ehrlich, J. Watras, Regulation of type 1 inositol 1,4,5-trisphosphate-gated calcium channels by InsP3 and calcium—simulation of single channel kinetics based on ligand binding and electrophysiological analysis, J. Gen. Physiol. 113 (1999) 837–849.

[15] C.E. Adkins, C.W. Taylor, Lateral inhibition of inositol 1,4,5-triphosphate receptors by cytosolic Ca^{2+}, Curr. Biol. 9 (1999) R1115–R1118.

[16] M. Bootman, P. Lipp, Calcium signalling: ringing changes to the 'bell-shaped curve', Curr. Biol. 9 (1999) R876–R878.

[17] D.-O.D. Mak, S. McBride, J.K. Foskett, Novel regulation of calcium inhibition of inositol 1,4,5-trisphosphate (InsP3) receptor (InsP3R) channel gating, J. Gen. Physiol., in press.

[18] L. Missiaen, H. De Smedt, J.B. Parys, R. Casteels, Co-activation of inositol trisphosphate-induced Ca^{2+} release by cytosolic Ca^{2+} is loading-dependent, J. Biol. Chem. 166 (1993) 461–473.

[19] I. Bezprozvanny, B.E. Ehrlich, Inositol (1,4,5)-trisphosphate InsP2-gated Ca channels from cerebellum: conduction properties for divalent cations and regulation by intraluminal calcium, J. Gen. Physiol. 104 (1994) 821–856.

[20] E.C. Thrower, H. Mobasheri, S. Dargan, P. Marius, E.J.A. Lea, A. Dawson, Interaction of luminal calcium and cytosolic ATP in the control of type 1 inositol (1,4,5)-trisphosphate receptor channels, J. Biol. Chem. 275 (2000) 36049–36055.

[21] I. Bezprozvanny, Theoretical analysis of calcium wave propagation based on inositol (1,4,5)-trisphosphate (IP3) receptor functional properties, Cell Calcium 16 (1994) 151–166.

[22] H.G. Othmer, Y. Tang, Oscillations and waves in a model of IP3-controlled calcium dynamics, in: Experimental and theoretical advances in biological pattern formation, Plenum Press, New York, 1993, pp. 277–299.

[23] C.W. Taylor, Inositol triphosphate receptors: Ca^{2+} modulated intracellular Ca^{2+} channels, Biochim. Biophys. Acta 1436 (1/2) (1994) 19–33.

[24] D. Colquhoun, B. Sakmann, Fast events in single-channel currents activated by acetylcholine and its analogues at the frog-muscle end-plate, J. Physiol. 369 (1985) 501–557.

[25] D.-O.D. Mak, S. McBride, J.K. Foskett, Spontaneous, ligand-independent channel activities of inositol 1,4,5-trisphosphate (InsP3) receptor (InsP3R), J. Gen. Physiol., in press.

[26] D.-O.D. Mak, S. McBride, J.K. Foskett, ATP regulation of type 1 inositol 1,4,5-trisphosphate receptor channel gating by allosteric tuning of Ca^{2+} activation, J. Biol. Chem. 274 (1999) 22231–22237.

[27] H. Tu, E. Nosyreva, T. Miyakawa, Z. Wang, A. Mizushima, M. Iino, I. Bezprozvanny, Functional and biochemical analysis of the type 1 inositol (1,4,5)-trisphosphate receptor calcium sensor, Biophys. J. 85 (2003) 290–299.

[28] D.-O.D. Mak, S. McBride, J.K. Foskett, ATP-dependent adenophostin activation of inositol 1,4,5-trisphosphate receptor channel gating, J. Gen. Physiol. 117 (2001) 299–314.

[29] D. Fraiman, S. Ponce Dawson, A solution for non constant mean open time in homogeneous Markov models, Physica A 32 (2003) 162–167.

[30] R.E. Hagar, B.E. Ehrlich, Regulation of the type III InsP-3 receptor by InsP3 and ATP, Biophys. J. 79 (1998) 271–278.

[31] J. Yang, S. McBride, D.-O.D. Mak, N. Vardi, K. Palczewski, F. Haeseleer, J.K. Foskett, Identification of a family of calcium sensors as protein ligands of inositol trisphosphate receptor Ca^{2+} release channels, Proc. Natl. Acad. Sci. U.S.A. 99 (2002) 7711–7716.

[32] M. Iino, M. Endo, Calcium-dependent immediate feedback control of inositol 1,4,5-triphosphate-induced Ca release, Nature 360 (1992) 76–78.

[33] I. Parker, J. Choi, Y. Yao, Elementary events of InsP(3)-induced Ca^{2+} liberation in xen oocytes: hot spots, puffs and blips, Cell Calcium 20 (1996) 105–121.

[34] E.A. Finch, G.J. Augustine, Local calcium singalling by inositol-1,4,5-triphosphate in Purkinje cell dendrites, Nature 396 (1998) 753–756.

[35] N. Callamaras, I. Parker, Phasic characteristic of elementary Ca release sites underlies quantal responses of IP3, EMBO J. 19 (2000) 3608–3617.

[36] T. Nguyen, W.-C. Chin, P. Verdugo, Role of Ca^{2+}/K^{+} ion exchange in intracellular storage and release of Ca^{2+}, Nature 395 (1998) 908–912.